

Simultaneous Purification of Round and Elongated Spermatids from Testis Tissue Using a FACS-Based DNA Ploidy Assay

R.B. Struijk,¹ C.M. De Winter-Korver,¹ S.K.M. van Daalen,¹ B. Hooibrink,² S. Repping,¹ A.M.M. van Pelt^{1*}

¹Center for Reproductive Medicine, Research Institute Reproduction and Development, Amsterdam UMC, University of Amsterdam, Amsterdam, The Netherlands

²Core Facility Cellular Imaging/LCAM-AMC, Department of Medical Biology, Amsterdam UMC, University of Amsterdam, Amsterdam, The Netherlands

Received 3 September 2018; Revised 9 November 2018; Accepted 21 November 2018

Grant sponsor: ZonMw, Grant number: TAS-116003002

Additional Supporting Information may be found in the online version of this article.

*Correspondence to: Prof. Dr. A.M.M. (Ans) van Pelt, Address: Meibergdreef 9-15, 1105AZ Amsterdam, The Netherlands
Email: a.m.vanpelt@amc.uva.nl

Published online 19 December 2018 in Wiley Online Library (wileyonlinelibrary.com)

DOI: 10.1002/cyto.a.23698

© 2018 The Authors. *Cytometry Part A* published by Wiley Periodicals, Inc. on behalf of International Society for Advancement of Cytometry.

This is an open access article under the terms of the Creative Commons Attribution-NonCommercial License, which permits use, distribution and reproduction in any medium, provided the original work is properly cited and is not used for commercial purposes.

• Abstract

Spermiogenesis is the final phase of spermatogenesis during which post-meiotic haploid round spermatids (rSpt) differentiate into elongated spermatozoa and includes several critical cell-specific processes like DNA condensation, formation of the acrosome, and production of the flagellum. Disturbances in this process will lead to complications in sperm development and subsequently cause infertility. As such, studying spermiogenesis has clinical relevance in investigating the etiology of male infertility and will improve our scientific understanding of male germ cell formation. Here, we were able to purify round spermatid and elongated spermatid fractions from a single cryopreserved human testicular tissues sample with an efficiency of $85.4\% \pm 4.9\%$ and $97.6\% \pm 0.6\%$, respectively. We confirmed the cell types by morphology and immunohistochemistry for histone H4 and PNA protein expression. The purity was measured by manual counting of histone H4 positive (round) and negative (elongated) spermatids in both sorted 1 N cell fractions. This method can be applied to both human and rodent studies. Especially in studies with limited access to testicular tissue, this method provides a reliable means to simultaneously isolate these cell types with high purity. Our method allows for further investigation of germ cell development and the process of spermiogenesis in particular, as well as provides a tool to study the etiology of male infertility, including morphological and biochemical assessment of round and elongating spermatids from subfertile men. © 2018 The Authors. *Cytometry Part A* published by Wiley Periodicals, Inc. on behalf of International Society for Advancement of Cytometry.

• Key terms

spermatogenesis; spermatids; post-meiosis; infertility; simultaneous cell sorting

SPERMATOGENESIS is the developmental process during which elongated spermatids are formed from spermatogonial stem cells (1). This process can be divided in three main steps: mitosis, meiosis, and spermiogenesis (2). Spermiogenesis is the final phase of spermatogenesis where post-meiotic haploid round spermatids (rSpt) differentiate into elongated spermatozoa (eSpt). During this maturation phase a number of crucial cell remodeling events are completed, including DNA condensation in the spermatid nucleus, formation of the acrosome, mitochondrial reorganization, production of the flagellum, and removal of cytoplasm (3–5). Aberrant spermiogenesis can result in abnormal acrosome development or various forms of developmental arrest, ultimately leading to infertility (6,7). As such, studying the process of spermiogenesis has clinical relevance in investigating the etiology of male infertility and will improve our scientific understanding of male germ cell formation (8). Effective and specific isolation of pure populations of germ cell types at different developmental steps is essential in reproductive studies and several protocols exist to purify these cells using different techniques, such as separation based on cell density

by Percoll gradient centrifugation (9) or STA-PUT velocity sedimentation (10–12) and separation based on DNA content analysis by FACS, utilizing DNA-intercalating dyes such as propidium iodide (PI), Hoechst 33342, or 4',6-diamidino-2-phenylindole (DAPI) (13,14). Typically, FACS methods using only intercalating DNA dyes are not sufficient to separate round from elongated spermatids as both have the same DNA content, while the efficacy of isolating pure germ cell populations through gradient separation methods is hampered by the inherent restriction of sorting cells based on cellular density, not DNA content. In this study, we identified two distinct peaks in the 1 N range of the DNA ploidy diagram that both include intact cells and not debris, which we confirm to consist of round and elongating spermatids based on morphological characterization and immunohistochemical stainings for histone H4 and peanut agglutinin (PNA) markers.

METHODS

Testicular Samples

Human testicular tissue fragments were obtained with informed consent from prostate cancer patients that underwent bilateral orchidectomy as part of their prostate cancer treatment. Testis from sexually mature mice and rats were obtained from various previous studies, that were approved according to the European legislation of animal experiments and were evaluated and approved by the Animal Ethic Committee of the Academic Medical Center, Amsterdam. Histological examination revealed full spermatogenesis in all testicular samples used, based on the presence of germ cells from all stages of development in the seminiferous tubules. Human testicular testis fragments of approximately 300–400 μ L (1 whole testes per vial for mouse, 1/8 parts of whole testes per vial for rat) were cryopreserved in 1 \times MEM (Minimal Essential Medium, Gibco, cat no. 21430-020) supplemented with 8% DMSO (dimethyl sulfoxide) and 20% FCS (fetal calf serum European approved origin, Gibco, cat no. 10270-106) using a slow freezing protocol and stored in liquid nitrogen vapor until further use.

Germ Cell Isolation from Cryopreserved Testicular Tissue

Germ cells were isolated from cryopreserved testicular tissues (human, mouse, and rat) using the following protocol: after thawing, the testicular biopsy was rinsed in sterile 1 \times PBS and put in a petri dish containing 8 mL phenol-free HTF medium (IVF basics, cat no. BE02-037F). Two microlance needles were used to dissociate the tissue followed by scraping of the tubules, in order to dislodge the cellular content. Next, the entire volume containing the tissue remains and cells was transferred to a clean 15 mL sterile tube and vigorously pipetted for several minutes using a 5 mL pipet. The suspension was then filtered through a 55 μ m mesh filter and the resulting suspension was centrifuged for 30 min at 4000g with break. The supernatant was removed and the pellet resuspended in 500 μ L to 1 mL 1 \times PBS depending on the

volume of the starting material. A 1.5 mL eppendorf tube was pre-rinsed with 1 \times MEM containing 20% FCS and the suspension was transferred to the tube, followed by a second centrifugation step at 4000g for 10 min in a swing-out centrifuge. Again, the supernatant was removed and the pellet was resuspended in 300 μ L cold 1 \times PBS. Then, a total volume of 700 μ L ice-cold 100% ethanol was added gradually to a final concentration of 70% ethanol/PBS, after which the cells were stored at 4°C until further use.

FACS

Fixed cells were centrifuged at 4165g for 15 min in a pre-cooled centrifuge and the supernatant was carefully decanted. Cells were permeabilized in 300 μ L permeabilization buffer (1 \times PBS containing 0.5% Triton-X) for 10 min at room temperature, washed with 1 \times PBS containing 1% BSA (bovine serum albumin fraction V, Roche, cat no. 10735094001) and centrifuged at 4165g for 10 min. Then, cells were labeled with 1 μ g/1 \times 10⁵ cells propidium iodide (PI, Sigma, P4964) in FACS/EDTA buffer (1 \times PBS with 1% FCS/0.1% NaN₃/2 mM EDTA) containing DNase-free RNase A (v/v 1:20) for 5 min. Finally, cells were filtered through a 50 μ m filter, collected in a 5 mL FACS tube, and put on ice. FACS measurements and sorting were performed on a Sony SH800Z cell Sorter (Sony Biotechnology Inc. Japan). Analysis of flow cytometry data and generation of figures was performed using FlowJo software version 10. A two-step gating check was performed in all samples to identify cells of interest within the normal size and granularity range (FSC-A/SSC-A) and to remove doublets from further analysis (FSC-H/FSC-W).

Sample Preparation for Immunohistochemistry

Paraffinized testicular tissue slices were deparaffinized using a standard rehydration protocol and washed in demineralized H₂O. After washing, tissue sections were boiled in 0.01 M sodium citrate buffer (tri-sodiumcitrate dihydrate C₆H₅Na₃O₇ · 2H₂O, pH 6.0) for 20 min to retrieve antigens.

The FACS sorted, PI labeled testicular cell suspensions were diluted in 1 \times PBS/1%BSA to a final concentration of 2.5 \times 10⁴ cells/100 μ L and loaded onto a glass slide via centrifugation at 20g for 5 min via a cytospin procedure. The slides were dried for 10 min at room temperature and fixated in freshly prepared 80% methanol/PBS solution for 10 min at –20°C, after which the slides were stored in 1 \times PBS at 4°C. At the day of the IHC experiment, slides were washed two times in 1 \times PBS while slowly shaking on a rotator, permeabilized by incubating the slides in 1 \times PBS/0.2% Triton X-100 for 10 min at room temperature and finally washed three times in 1 \times PBS.

Whole testis tissue slides and FACS sorted cells prepared for IHC were stained for histone H4 protein using anti-histone H4 antibody (Supporting Information Table S1) and the following IHC protocol; tissue slides and cytospins were incubated with freshly prepared endogenous peroxidase blocking solution (1 \times PBS/0.3% H₂O₂) for 10 min at room temperature. Slides were then washed three times with 1 \times PBS and incubated with 100 μ L Superblock (ScyTek

Laboratories, cat no. AAA999) for 1 h to block non-specific antibody binding, followed by overnight incubation at 4°C with anti-Histone H4 antibody diluted 1:300 in Normal Antibody Diluent (IL Immunologic, cat no. BD09-999). The following day, slides were washed three times in 1× PBS and incubated for 30 min at room temperature with 100 µL Powervision Poly-Hrp-anti Ms/Rb secondary antibody (IL Immunologic, cat no. VWRKDPVO110HRP). Subsequently, slides were incubated with demineralized H₂O containing 0.5 mg/mL DAB and 1% H₂O₂ for 4 min and placed in 1 × PBS directly after. Finally, slides were dehydrated sequentially with 70%/96%/100% ethanol and xylene and encapsulated with a cover slip using Entellan (Merck, cat no. 1079610100). For acrosome detection, cells were incubated with 0.5 µg/mL of the lectin peanut agglutinin (PNA) conjugated with Alexa Fluor 488 conjugate (L21409, Life Technologies, Supporting Information Table S2) and nuclear counterstaining with 0.2 µg/mL DAPI and embedded in Prolong Gold.

Microscopy

Microscopy data included in this article for histone H4 was acquired using an Olympus BX41 microscope (Olympus America, USA) and Leica DMC4500 camera (Leica Microsystems). High resolution images were captured at 2560 × 1920 resolution and adjusted using the following settings: Gain 1.0; Color-correct-red 1.0; Color-correct-green 1.49; Color-correct-blue 2.9; Brightness-level 188.5; and Color-saturation 150. Histological images of PNA-488 acrosome staining were acquired using the Leica DM 5000B microscope and Leica DFC365FX camera. Images were captured at resolution 8 and adapted using LAS AF software.

Statistics and Counting

Counting experiments were performed by manual counting of the number of H4-positive (round) and H4-negative (elongated, compacted) cells in each sample using sequentially recorded images of the cytospin area, moving the camera from left to right, top to bottom by a fixed distance. The purity values displayed in Figure 1C were calculated as the average percentage of H4-positive cells per group of samples ($n = 3$) ± standard error of the mean (SEM).

RESULTS

We first attempted to isolate both the haploid (1 N) and diploid (2 N) germ cell populations from cryopreserved human testicular tissues using PI staining and observed two distinct populations of cells in the 1 N range with similar forward scatter/side scatter (FSC/SSC) parameters (Fig. 1A and Supporting Information Fig. S1). Based on previous studies detailing the DNA content of various testicular germ cell populations (15,16) we hypothesized that these two populations might represent round and elongated spermatids, respectively, since both are haploid but differ from each other in terms of DNA compaction. Indeed, when we sorted both populations (termed “sub1N” and “1 N” based on PI signal)

and loaded the obtained cell fractions onto glass slides via cytospin, we morphologically observed a high percentage of cells in the sub1N-sorted fraction that displayed phenotypical characteristics of elongated spermatids (oval-shaped, highly condensed nucleus) and, vice versa, a high percentage of cells in the 1 N-sorted cell fraction that displayed characteristics of round spermatids (round nucleus). To further investigate the purity of the obtained cell fractions, we investigated the expression of histone H4 (H4) protein in the sorted cell fractions. Histone H4 is one of the core nucleosome proteins, that is expressed in most human cells and functions in chromatin structuring and DNA accessibility (17). During mammalian spermiogenesis, nuclear histones are sequentially replaced by protamines in a process called histone-to-protamine transition to facilitate chromatin hyper-compaction (18). Due to this testis-specific process, histone H4 protein is expressed at high levels in all testicular cells excluding elongating spermatids, which show severely reduced levels of histone H4 protein hardly detectable by immunohistochemistry (Supporting Information Fig. S2). We immuno-stained the sorted cell fractions for H4 and observed a distinct lack of H4 protein in the sub1N population, while the 1 N population almost uniformly expressed H4 protein (Fig. 1B). Next, we determined the percentage of H4-negative cells in the sub1N population and the percentage of H4-positive cells in the 1 N population from human testicular cell suspensions of three non-related donors by manual counting of sorted cell fractions mounted on glass slides and stained for histone H4 using immunohistochemistry (see Methods). An average of 215.85 ± 19.98 cells was counted per sample and visually scored for histone H4 positive (round) and negative (elongating) spermatids (Supporting Information Table S3). This revealed high degrees of purity for both the sub1N fraction ($97.6\% \pm 0.6\%$ H4-negative) and 1 N fraction ($85.4\% \pm 4.9\%$ H4-positive) (Fig. 1C). We further confirmed that the 1 N fraction contains round spermatids by staining the acrosome with peanut agglutinin (PNA) (Supporting Information Fig. S3). We then examined whether this purification method also worked in mouse and rat. We confirmed a purity of H4-negative cells in the sub1N fraction of $60.3\% \pm 5.8\%$ and $89.3\% \pm 0.8\%$ in mouse ($n = 3$) and rat ($n = 3$), respectively, while the corresponding purity of H4-positive cells in the 1 N fraction was $95.2\% \pm 1.5\%$ and $94.1\% \pm 3.1\%$ (Fig. 1C, also see Supporting Information Table S3 and Fig. S2).

DISCUSSION

In this report, we describe an effective and simple method to simultaneously purify round and elongated spermatids from testis material of human, rat and mouse using the DNA intercalating dye PI. The observation of 2 peaks in the 1 N range was clearly visible when sorting for human spermatids and further characterization revealed distinct populations of round and elongating spermatids. This was further confirmed by the high percentage of positive H4 cells in the H4 fraction and the low percentage in the sub1N fraction. We suspect that the lower purity of elongating

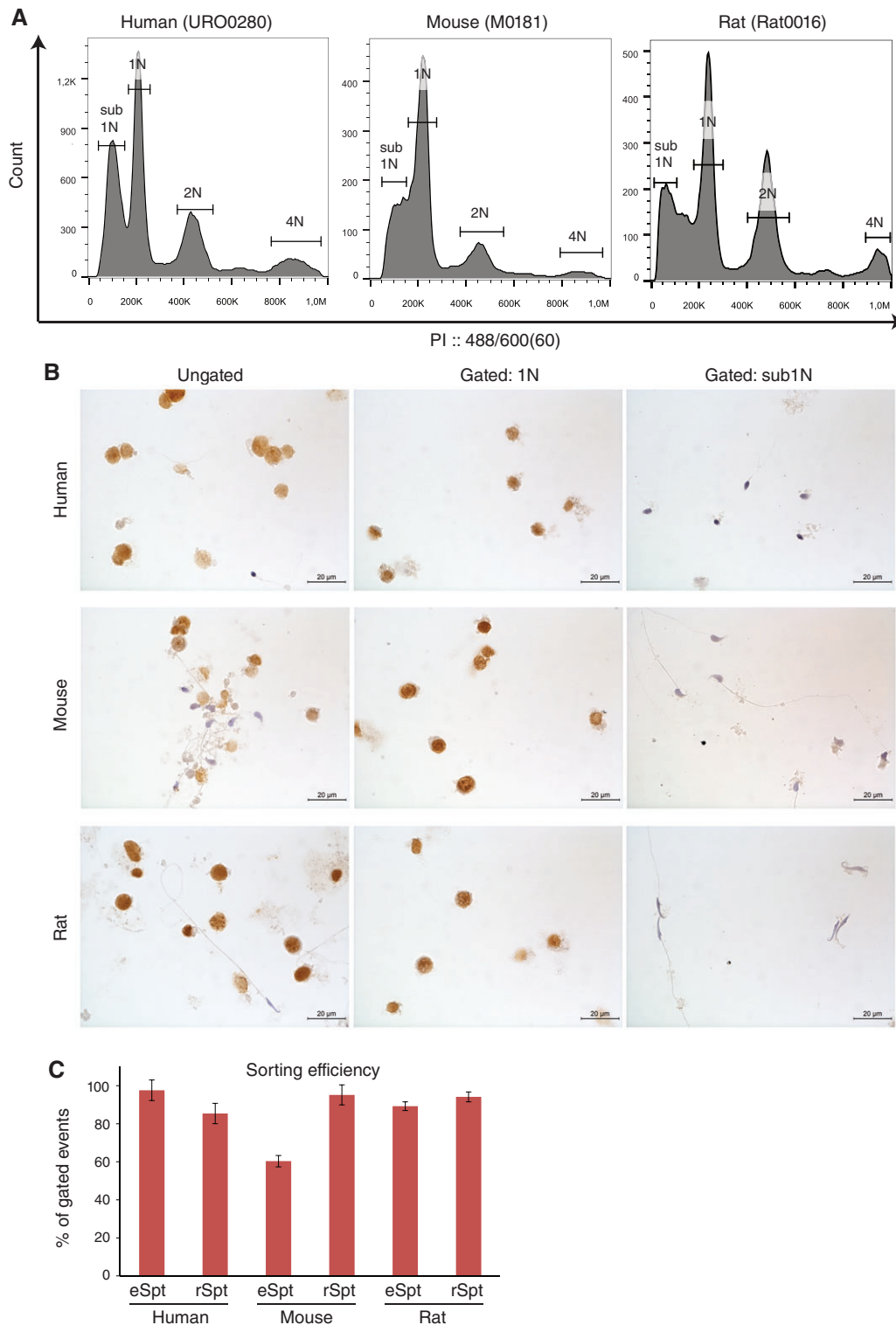


Figure 1. FACS is sufficient to isolate simultaneously pure populations of round and elongated spermatids. (A) Representative DNA ploidy histograms stained with PI for human, mouse and rat mixed cell fractions isolated from cryopreserved testicular tissue. (B) Immunohistochemistry staining of the unsorted and sorted cell fractions for histone 4 (H4). These cytospin slides were used to determine the purity of the sorted 1 N fractions in each sample. (C) Purity of the FACS-sorted germ cell fractions for human, rat and mouse sorting (“h,” “r,” and “m” affixes). Bars display the average number of histone H4-negative cells in the sub1N sorted population (eSpt) and the average number of histone H4-positive cells in the 1 N sorted population (rSpt). Whiskers indicate standard error of the mean.

spermatids in the sub1N peak in mice is related to the larger shape of the elongating sperm head, which could be more easily accessible to PI in mice as compared with humans and rats and thereby resulting in a higher overlap with the 1 N peak. Although we used a testicular cell isolation method of scraping of seminiferous tubules from testicular tissue, adapted from the testicular sperm extraction (TESE) method routinely used in clinical IVF practice, we believe that cell isolation with enzymatic digestion of the testicular will also reveal separation of both 1 N and sub 1 N cells.

The method we describe here for cell sorting is potentially relevant to study the processes that occur during normal spermiogenesis as well as cases in which spermiogenesis is disturbed. The main advantage of our method over existing protocols is that it combines separation of cells based on both cellular density and DNA content and allows for sorting of cells isolated from cryopreserved testicular tissues. Furthermore, our method could be expanded to include other spermatid specific markers to distinguish more detailed characteristics of the round and elongating spermatid populations, also in a simultaneous manner. Finally, the protocol could be adapted to allow for nucleic acid studies in the isolated spermatid populations if some adjustments are made in terms of DNA/RNA content preservation, for example, by utilizing RNase inhibitors and proteinases during sample work-up.

CONCLUSIONS

In conclusion, we here provide an effective and simple FACS method based on the DNA intercalating dye PI to simultaneously purify populations of round and elongated spermatids from human or rat testis, as well as a pure population of round spermatids from mouse testis. This method is highly reproducible, with a purification efficiency of $\geq 85\%$ in humans. This protocol can aid in unraveling fundamental questions regarding human and rodent spermiogenesis, as well as provide a tool to study the etiology of male infertility, including morphological and biochemical analyses of round and elongating spermatids from subfertile men with normal sperm counts.

ACKNOWLEDGMENT

We would like to thank all members of the Core Facility Cellular Imaging (Department of Medical Biology, AMC Amsterdam) for technical assistance with the FACS experiments.

LITERATURE CITED

1. de Rooij DG. The nature and dynamics of spermatogonial stem cells. *Development* 2017;144:3022–3030.
2. Griswold MD. Spermatogenesis: The commitment to meiosis. *Physiol Rev* 2016; 96:1–17.
3. Jan SZ, Hamer G, Repping S, de Rooij DG, van Pelt AM, Vormer TL. Molecular control of rodent spermatogenesis. *Biochim Biophys Acta* 2012;1822:1838–1850.
4. Dunleavy JEM, Okuda H, O'Connor AE, Merriner DJ, O'Donnell L, Jamsai D, Bergmann M, O'Bryan MK. Katanin-like 2 (KATNAL2) functions in multiple aspects of haploid male germ cell development in the mouse. *PLoS Genet* 2017;13:e1007078.
5. Wei YL, Yang WX. The acroframosome-acroplaxome-manchette axis may function in sperm head shaping and male fertility. *Gene* 2018;660:28–40.
6. O'Donnell L. Mechanisms of spermiogenesis and spermiation and how they are disturbed. *Spermatogenesis* 2014;4:e979623.
7. Chemes HE, Rawe VY. The making of abnormal spermatozoa: Cellular and molecular mechanisms underlying pathological spermiogenesis. *Cell Tissue Res* 2010;341: 349–357.
8. Sanchez V, Wistuba J, Mallidis C. Semen analysis: Update on clinical value, current needs and future perspectives. *Reproduction* 2013;146:R249–R258.
9. Gandini L, Lenzi A, Lombardo F, Pacifici R, Dondero F. Immature germ cell separation using a modified discontinuous Percoll gradient technique in human semen. *Hum Reprod* 1999;14:1022–1027.
10. Liu Y, Niu M, Yao C, Hai Y, Yuan Q, Liu Y, Guo Y, Li Z, He Z. Fractionation of human spermatogenic cells using STA-PUT gravity sedimentation and their miRNA profiling. *Sci Rep* 2015;5:8084.
11. Bryant JM, Meyer-Ficca ML, Dang VM, Berger SL, Meyer RG. Separation of spermatogenic cell types using STA-PUT velocity sedimentation. *J Vis Exp* 2013;9:80.
12. Miller RG, Phillips RA. Separation of cells by velocity sedimentation. *J Cell Physiol* 1969;73:191–201.
13. Hacker-Klom UB, Gohde W, Nieschlag E, Behre HM. DNA flow cytometry of human semen. *Hum Reprod* 1999;14:2506–2512.
14. Bastos H, Lassalle B, Chicheportiche A, Riou L, Testart J, Allemand I, Fouchet P. Flow cytometric characterization of viable meiotic and postmeiotic cells by Hoechst 33342 in mouse spermatogenesis. *Cytometry A* 2005;65:40–49.
15. Rodriguez-Casuriaga R, Geisinger A, Lopez-Carro B, Porro V, Wettstein R, Folle GA. Ultra-fast and optimized method for the preparation of rodent testicular cells for flow cytometric analysis. *Biol Proced Online* 2009;11:184–195.
16. Vigodner M, Lewy H, Lewin LM, Shochat L, Golan R. Evidence for biological rhythm in spermatogenesis in the pubertal hamster (*Mesocricetus auratus*): A flow cytometric study. *Life Sci* 2004;74:1119–1126.
17. Henikoff S, Smith MM. Histone variants and epigenetics. *Cold Spring Harb Perspect Biol* 2015;7:a019364.
18. Bao J, Bedford MT. Epigenetic regulation of the histone-to-protamine transition during spermiogenesis. *Reproduction* 2016;151:R55–R70.